IV. Conclusions

Useful oscillographic response plots of a microwave network have been obtained by computer simulation, using frequency-domain data measured with a computer-controlled network analyzer. The technique has a short time resolution, is highly sensitive, and provides quantitative results useful in a variety of ways. A major application is in the analysis of impedance data at the input of transmission networks, where it serves as a quantitatively interpretable time-domain reflectometer. It may also be used to measure small reflection coefficients of individual parts of multiple-section networks, which are physically inseparable both in the time domain and the frequency domain.

References

[1] D. L. Hollway, "The comparison reflectometer," *IEEE Trans. Microwave Theory Tech.*, vol. MTT-15, pp. 250–259, Apr. 1967.

[2] P. I. Somlo, "The locating reflectometer," *IEEE Trans. Microwave Theory Tech.*, vol. MTT-20, pp. 105–112, Feb. 1972.

[3] L. A. Robinson, W. B. Weir, and L. Young, "An RF time-domain reflectometer not in real time," *IEEE Trans. Microwave Theory Tech.* (*1972 Symposium Issue*), vol. MTT-20, pp. 855–857, Dec. 1972.

[4] A. M. Nicolson, C. L. Bennett, Jr., D. Lamensdorf, and L. Susman, "Applications of time-domain metrology to the automation of broad-band microwave measurements," *IEEE Trans. Microwave Theory Tech.* (*Special Issue on Automated Microwave Measurements*), vol. MTT-20, pp. 3–9, Jan. 1972.

De-Embedding and Unterminating

RONALD F. BAUER, MEMBER, IEEE, AND PAUL PENFIELD, JR., FELLOW, IEEE

***Abstract*—De-embedding is the process of deducing the impedance of a device under test from measurements made at a distance, when the electrical properties of the intervening structure are known. Unterminating is the process of deducing the electrical properties of the intervening structure from a series of measurements with known embedded devices. The mathematical steps necessary for de-embedding and unterminating are reviewed, and a technique is presented for unterminating with theoretically redundant measurements in order to minimize the effect of experimental errors.**

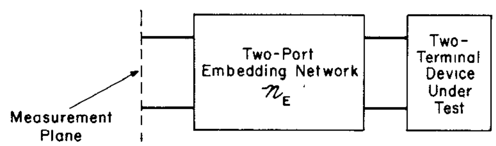

Fig. 1. Normal measurement situation. Characteristics of the device under test can only be measured as they appear outside the embedding network $\mathfrak{N}_E$.

I. Introduction

At microwave frequencies it is often impossible to directly measure the impedance (or admittance or reflection coefficient) of devices such as diodes or transistors. Instead, measurements are made at, and referred to, some reference plane physically removed from the device. The device is then said to be "embedded" in the intervening structure. If the device under test is a two-terminal device, then the "embedding network" may usefully be regarded as a two-port network $\mathfrak{N}_E$, with the measurement plane at the input and the device under test terminating the output. This is shown in Fig. 1.

A related problem is that of characterizing, for a working circuit, the region surrounding a device such as a diode. For example, one might wish to know the impedance seen by the diode, or the coupling between the diode and the circuit input or output. It is often impossible to make measurements at the physical location of the device, so what is needed is a characterization of the structure between the device and a convenient measurement plane. Again it is useful to consider the device as "embedded" in the intervening structure, which in the case of a diode may be regarded as a two-port network $\mathfrak{N}_E$. Fig. 1 is again relevant.

To fix ideas in this paper, we shall consider mainly impedance (instead of admittance or reflection coefficient) measurements, and call the device under test a "diode."

There are two distinct problems. One is, given the measured impedance at the input of the two-port network, to deduce the impedance of the diode. This process, known as "de-embedding," is straightforward, once the embedding network is known, and is discussed in Section II. The other more difficult problem is to characterize the

Manuscript received July 30, 1973; revised October 18, 1973. This work was supported by the Department of the Air Force.

R. F. Bauer is with the M.I.T. Lincoln Laboratory, Lexington, Massachusetts 02173.

P. Penfield, Jr., is a Consultant at the M.I.T. Lincoln Laboratory, Lexington, Massachusetts 02173, and is with the Department of Electrical Engineering and Research Laboratory of Electronics, Massachusetts Institute of Technology, Cambridge, Massachusetts.

embedding network $\mathcal{N}_E$ experimentally from measurements. Because measurements at the output of $\mathcal{N}_E$ are impossible, this characterization must be done from measurements of input impedance alone, made when $\mathcal{N}_E$ is terminated by known loads at the output. The process, known as "unterminating," is discussed in Sections III–VIII.

II. De-Embedding

The de-embedding procedure is straightforward, provided the embedding network is known. Let us suppose a load with unknown impedance Z_L terminates the output of the embedding network, and the resulting input impedance Z_{IN} is measured.

One direct way to de-embed is to solve the well-known formula for input impedance

$$Z_{IN} = Z_{11} - \frac{Z_{12}Z_{21}}{Z_{22} + Z_L} \tag{1}$$

for the unknown Z_L:

$$Z_L = \frac{Z_{12}Z_{21}}{Z_{11} - Z_{IN}} - Z_{22}. \tag{2}$$

Similar formulas can easily be derived for admittance or reflection coefficient.

A convenient way to view the process is to imagine the original network $\mathcal{N}_E$, as terminated, forming the termination of a hypothetical two-port network $\mathcal{N}_I$, as in Fig. 2. If $\mathcal{N}_I$ is the inverse of $\mathcal{N}_E$ with respect to cascading, then the resulting input impedance is equal to Z_L. This inverse network is easily found if $\mathcal{N}_E$ is known. In terms of the *ABCD* parameters, $\mathcal{N}_I$ has an *ABCD* matrix equal to the matrix inverse of the *ABCD* matrix of $\mathcal{N}_E$. The impedance matrix of $\mathcal{N}_I$ is found by multiplying by -1 and replacing subscripts 1 by 2 and vice versa. In MARTHA notation [1], if the original embedding network is denoted NE, then $\mathcal{N}_I$ is (-1) ZSCALE WN NE.

III. Unterminating

In principle there are many ways of characterizing the two-port embedding network. In practice the most common are: (1) a lumped and/or distributed equivalent circuit; (2) analytical expressions for the two-port parameters, perhaps found through solving Maxwell's equations; (3) analytical or polynomial approximations for the two-port parameters; (4) measured numerical values for the two-port parameters, typically in the form of a table with entries at several frequencies; and (5) two or more such networks wired together.

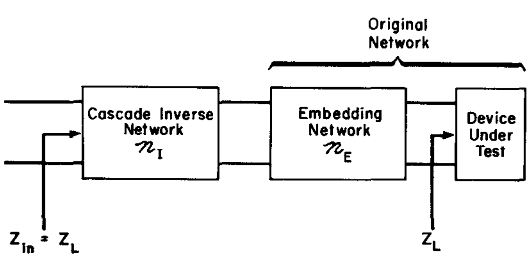

Fig. 2. When $\mathcal{N}_I$ is the cascade inverse of the embedding network $\mathcal{N}_E$, then the input impedance is the device impedance.

In this paper we discuss a technique, known as "unterminating," to deduce numerical values for the two-port parameters from measurements made solely at the input of the embedding network. This technique has both theoretical and practical limitations. A technique is described for utilizing theoretically redundant information to improve accuracy. A similar approach, but restricted to the case where the variable load impedance is purely reactive, was used by Kajfez [2], who was particularly interested in the de-embedding of varactors. It should be noted that when (as in the case considered by Kajfez) the variable load is reactive, the locus of input impedance is a circle in the complex plane, whereas in the general case (considered here) the locus need not be a circle. Thus this technique is applicable in cases where "eyeball" fitting of a circle is not a possible technique.

IV. Theoretical Basis and Fundamental Limitations

To fix ideas consider the impedance matrix of the embedding network $\mathcal{N}_E$, with elements Z_{11}, Z_{12}, Z_{21}, and Z_{22}. The network need not be lossless, passive, or reciprocal.

The technique for unterminating is based on (1), which can also be written as

$$Z_{IN} = \frac{\Delta_Z + Z_{11}Z_L}{Z_{22} + Z_L} \tag{3}$$

where $\Delta_Z = Z_{11}Z_{22} - Z_{12}Z_{21}$. The unterminating procedure is to measure Z_{IN} as a function of frequency for a set of known load impedances Z_L, and then deduce Z_{11}, Z_{22}, and Δ_Z. Two or fewer measurements are insufficient; three independent measurements are necessary and sufficient; and four or more measurements are redundant. It is a simple algebraic task to find explicit formulas for Z_{11}, Z_{22}, and Δ_Z from (3) for three independent pairs (Z_{IN1}, Z_{L1}), (Z_{IN2}, Z_{L2}), and (Z_{IN3}, Z_{L3}). However, use of these formulas is *not recommended* since it is difficult to avoid the effects of experimental errors. A technique to utilize redundant measurements to reduce experimental error is discussed in Section VI.

Although a two-port network has four elements in its impedance matrix, the two elements Z_{12} and Z_{21} appear in (1) only in the form of the product $Z_{12}Z_{21}$. Driving-point measurements of a terminated two-port network are inherently incapable of determining separately Z_{12} and Z_{21}. If $\mathcal{N}_E$ is known to be reciprocal, then $Z_{12} = Z_{21}$ and, except for a sign ambiguity, Z_{12} and Z_{21} can be determined. The physical effect of this sign ambiguity is illustrated in Fig. 3. If one choice of sign corresponds to a network $\mathcal{N}$, then the other choice corresponds to the network $\mathcal{N}$ cascaded with a polarity reverser. It is obvious that these two networks cannot be distinguished on the basis of driving-point measurements.

On the other hand, if the embedding network is nonreciprocal, not even the magnitudes of Z_{12} and Z_{21} can be

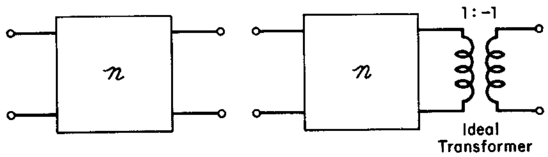

Fig. 3. Effect of sign ambiguity in Z_{12} and Z_{21}, if only the product $Z_{12}Z_{21}$ is known. Both of the networks above are reciprocal, but differ in the sign of Z_{12} and Z_{21}.

determined without some assumption. Fortunately, however, the inherent impossibility of finding separately Z_{12} and Z_{21} does not affect the use of the resulting network for de-embedding or determining output impedance, as can be seen from Z_L expressed in terms of Z_{IN}, and Z_{OUT} expressed in terms of the generator impedance Z_G:

$$Z_L = -Z_{22} + \frac{Z_{12}Z_{21}}{Z_{11} - Z_{\text{IN}}} = \frac{-\Delta_Z + Z_{22}Z_{\text{IN}}}{Z_{11} - Z_{\text{IN}}} \tag{4}$$

$$Z_{\text{OUT}} = Z_{22} - \frac{Z_{12}Z_{21}}{Z_{11} + Z_G} = \frac{\Delta_Z + Z_{22}Z_G}{Z_{11} + Z_G}. \tag{5}$$

In both forms only the product $Z_{12}Z_{21}$ appears. This means that any choice of Z_{12} and Z_{21} such that their product is correct, is adequate. It is usually convenient to choose $Z_{12} = Z_{21}$ even for nonreciprocal networks, and to choose the sign resulting from the square root arbitrarily. This means that (even for reciprocal networks) the resulting network is, or may be, wrong, but in such a way that de-embedding or determining the output impedance is still possible.

This technique requires knowledge of the loads at the time the input measurements are made. An important limitation of the procedure is the fact that the supposedly known loads often cannot be directly measured. Naturally, the success of the unterminating operation is only as good as the knowledge of the load impedances. For example, taking values for the set of load impedances that are consistently in error by an additive constant will introduce a fictitious element in series with the output port of the network defined by the untermination process. A set of load impedances consistently in error by a multiplicative constant will introduce a fictitious ideal transformer across the output port. In some cases there is no particular problem in determining the impedance of the reference loads (for example, using the back-bias capacitances of a diode, which are assumed to be the same as the capacitances measured as a lower frequency [3]). In other cases, however, some modeling effort must be taken (for example, substituting for a diode package a series of dielectric or conductive pieces with the same shape [4]), and care must be exercised in selecting the reference loads in order to preserve the desired bilinear relation between Z_{IN} and Z_L[5].

V. Effect of Experimental Error

It was stated above that three input measurements are necessary and sufficient for deducing the embedding network. However, when only three measurements are used, the technique is subject to difficulties arising from experimental error. The following simulated example shows how important such considerations are.

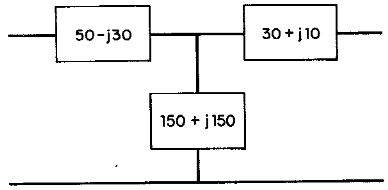

Fig. 4. Example embedding network. $Z_{11} = 200 + j120$, $Z_{22} = 180 + j160$, $Z_{12} = Z_{21} = 150 + j150$, $\Delta_Z = 16800 + j8600$.

TABLE I
Input Impedances Z_{IN} of the Example Embedding Network Fig. 4 When Terminated with Reference Loads Z_L and Input Impedances After Adding Noise

Z_L		Z_{IN}		Z_{IN} + Noise	
Real	Imag.	Real	Imag.	Real	Imag.
10	0	83.31	-18.57	82.58	-18.05
25	0	93.53	-16.41	93.45	-16.34
75	0	120.6	- 6.621	120	- 7.521
100	0	130.8	- 1.154	131.1	- 0.7938
0	50	76.47	14.12	77.34	13.89
00	-50	88.76	-62.02	88.8	-61.35
50	50	102.6	13.3	101.6	12.41
50	-50	123.8	-39.23	123.9	-38.88

The network shown in Fig. 4 was used as the embedding network. The input impedance was calculated at one frequency for eight different loads, namely, resistances of 10, 25, 75, and 100 Ω, reactances equal to $j50$ and $-j50$ Ω, and impedances of $50 + j50$ and $50 - j50$ Ω. To simulate experimental error each input impedance was perturbed by adding an independent random resistance and random reactance of maximum magnitude 1. The resulting "noisy measurements" are shown in Table I. For simplicity the eight load impedances were assumed to be known exactly.

Any three of the eight pairs of Z_L and "measured" Z_{IN} can be selected for unterminating. Since there are 56 ways of selecting 3 objects from a set of 8, there are 56 different approximations of the embedding network. Each of these was used to de-embed the input impedance $108.3 - j11.85$ Ω (which is the actual result of a 50-Ω load). The 56 resulting estimates of the load impedance $\hat{Z}_L$ are shown in Fig. 5. The scatter indicates the extent of the error introduced by measurement errors of less than 1 Ω. In a practical case it would not be evident which (if any) of the 56 resulting networks was best.

What is needed is some way of averaging over the extra measurements in order to improve the accuracy of the embedding network characterization. In Section VI such a technique is discussed. As a preview, the effect of using this technique is shown in Table II. The mean and standard deviation are given for the 56 load impedances predicted using the embedding networks derived by taking 3 measurements at a time, the 70 predictions derived by taking 4 out of the 8 measurements, the 56 predictions based on 5 measurements, the 28 predictions based on 6

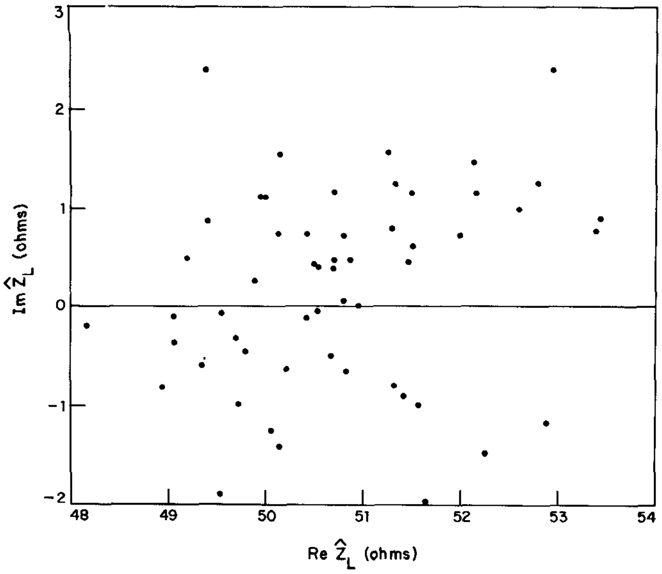

Fig. 5. Plot of the load impedances obtained by de-embedding the input impedance $108.3 - j11.8\ \Omega$ (Z_{IN} of the network in Fig. 4 terminated in $Z_L = 50$) using the 56 different descriptions of the embedding network obtained using 3 noisy measurements at a time from a set of 8.

TABLE II
AVERAGE AND STANDARD DEVIATION OF LOAD IMPEDANCES OBTAINED BY DE-EMBEDDING INPUT IMPEDANCE $108.3 - j11.8\ \Omega$, USING EMBEDDING NETWORKS OBTAINED USING N NOISY MEASUREMENTS AT A TIME FROM A SET OF EIGHT

N	Average Re Z_L	Average Im Z_L	Standard Deviation Re Z_L	Standard Deviation Im Z_L
3	50.80	.2116	1.199	1.1
4	50.63	.0408	0.7046	0.6462
5	50.51	.01328	0.5576	0.4175
6	50.42	-.007462	0.4303	0.2525
7	50.35	-.02279	0.2883	0.1167
8	50.30	-.03362		

measurements, the 8 predictions based on 7 measurements, and the 1 prediction based on all 8 measurements. It is apparent that as more measurements are used, the scatter decreases and the prediction of the load impedance becomes better.

VI. Recommended Untermination Procedure

The procedure for unterminating presented here makes use of *all* pairs of measurements and loads, with equal weighting of importance (although it can easily be modified to any desired unequal weighting). It is based on the minimization of an error expression to obtain estimates of the network parameters Z_{11}, Z_{22}, and Δ_Z. An error expression that is quadratic in these parameters is used in order to obtain explicit minimization formulas.

The error expression is derived by rearranging (3) to obtain a linear equation in Z_{11}, Z_{22}, and Δ_Z:

$$Z_{11}Z_L - Z_{22}Z_{IN} + \Delta_Z - Z_LZ_{IN} = 0. \quad (6)$$

For any particular measurement–load pair, (6) will differ from 0 by an amount ϵ_i due to measurement errors in Z_{INi} and/or uncertainty about the value of Z_{Li}. Thus for each of the N measurement–load pairs

$$Z_{11}Z_{Li} - Z_{22}Z_{INi} + \Delta_Z - Z_{Li}Z_{INi} = \epsilon_i, \quad (i = 1,2,3,\cdots,N). \quad (7)$$

An estimate of the network parameters can be obtained by choosing Z_{11}, Z_{22}, and Δ_Z to minimize the squared magnitudes of all expressions like (7). That is, the function

$$\boldsymbol{\varepsilon}'\boldsymbol{\varepsilon}^* = \sum_{i=1}^{N} |\epsilon_i|^2 = \sum_{i=1}^{N} |Z_{11}Z_{Li} - Z_{22}Z_{INi} + \Delta_Z - Z_{Li}Z_{INi}|^2 \quad (8)$$

is to be minimized.

This problem can be expressed in matrix form as

$$\boldsymbol{\beta}\boldsymbol{p} - \boldsymbol{\alpha} = \boldsymbol{\varepsilon} \quad (9)$$

where

$$\boldsymbol{p}' = [Z_{11} \quad Z_{22} \quad \Delta_Z]$$

$$\boldsymbol{\alpha}' = [Z_{L1}Z_{IN1} \quad Z_{L2}Z_{IN2} \quad \cdots \quad Z_{LN}Z_{INN}]$$

$$\boldsymbol{\beta} = \begin{bmatrix} Z_{L1} & -Z_{IN1} & 1 \\ Z_{L2} & -Z_{IN2} & 1 \\ \vdots & \vdots & \vdots \\ Z_{LN} & -Z_{INN} & 1 \end{bmatrix}$$

$$\boldsymbol{\varepsilon}' = [\epsilon_1 \quad \epsilon_2 \quad \cdots \quad \epsilon_N].$$

Then choosing for $\hat{\mathbf{p}}$, the parameter estimator, the value of $\boldsymbol{p}$ that minimizes $\boldsymbol{\varepsilon}'\boldsymbol{\varepsilon}^*$ gives

$$\boldsymbol{\beta}^{*\prime}\boldsymbol{\beta}\hat{\mathbf{p}} = \boldsymbol{\beta}^{*\prime}\boldsymbol{\alpha} \quad (10)$$

where

$$\boldsymbol{\beta}^{*\prime}\boldsymbol{\beta} = \begin{bmatrix} \sum_{i=1}^{N} |Z_{Li}|^2 & -\sum_{i=1}^{N} Z_{Li}^*Z_{INi} & \sum_{i=1}^{N} Z_{Li}^* \\ -\sum_{i=1}^{N} Z_{Li}Z_{INi}^* & \sum_{i=1}^{N} |Z_{INi}|^2 & -\sum_{i=1}^{N} Z_{INi}^* \\ \sum_{i=1}^{N} Z_{Li} & -\sum_{i=1}^{N} Z_{INi} & N \end{bmatrix} \quad (11)$$

and

$$\boldsymbol{\beta}^{*\prime}\boldsymbol{\alpha} = \begin{bmatrix} \sum_{i=1}^{N} |Z_{Li}|^2 Z_{INi} \\ -\sum_{i=1}^{N} |Z_{INi}|^2 Z_{Li} \\ \sum_{i=1}^{N} Z_{Li}Z_{INi} \end{bmatrix}. \quad (12)$$

Two algorithms for computing $\hat{Z}_{11}$, $\hat{Z}_{22}$, and $\hat{\Delta}_Z$ are shown in Fig. 6. They are written in the language APL and are intended for illustration only, although they can actually be executed for real load and input impedances (in that case the complex conjugate function CC is bypassed). Practical programs based on the algorithms in Fig. 6 are possible, but would be unnecessarily slow. It is a simple matter to devise alternate algorithms that are not as well suited for exposition, but better suited for actual calculations.

Our goal, however, is not just to estimate the network parameters. We would like to use them to estimate the expected value of Z_L from additional, or future, observations of $Z_{\rm IN}$, or to estimate the expected value of $Z_{\rm OUT}$. The equations for Z_L and $Z_{\rm OUT}$, (4) and (5), are nonlinear in the network parameters. Thus they will not be unbiased estimators. However, if the network parameters are known with a small enough variance the bias in the estimate of Z_L or $Z_{\rm OUT}$ should be small. An example of the use of this procedure is given in Section VIII.

VII. Extensions

This technique is also applicable to instances involving admittance and reflection coefficient. Indeed, the input admittance $Y_{\rm IN}$ as a function of the load admittance Y_L and admittance matrix is

$$Y_{\rm IN} = Y_{11} - \frac{Y_{12}Y_{21}}{Y_{22} + Y_L}. \tag{13}$$

This has exactly the same form as (1), and therefore the same procedure can be used without modification. In particular, if measured $Y_{\rm IN}$ and Y_L values are used as an argument for the function UNT in Fig. 6, the function will return the vector Y_{11}, Y_{22}, Δ_Y.

The extension to reflection coefficients is almost as easy. The input reflection coefficient $\Gamma_{\rm IN}$ in terms of the load reflection coefficient Γ_L and scattering matrix S is

$$\Gamma_{\rm IN} = S_{11} - \frac{S_{12}S_{21}}{S_{22} - 1/\Gamma_L} \tag{14}$$

which has a form similar to (1) except that $-1/\Gamma_L$ appears instead of Z_L. Thus the same function UNT can be used with reflection coefficient data provided that instead of Z_L, $-1/\Gamma_L$ is used. The data are probably most easily arranged as a vector of $\Gamma_{\rm IN}$ and Γ_L, but it is a simple matter to write a function such as FORS in Fig. 7 that can be used to precondition the argument. Then, if the vector DATA contains $\Gamma_{\rm IN}$ and Γ_L numbers, UNT FORS DATA will return a vector containing the scattering-matrix values S_{11}, S_{22}, and Δ_S. In the example in Section VIII, reflection coefficient data were actually used.

It is also possible to make use of data, if any, of output impedance (or admittance or reflection coefficient) for a given impedance Z_G terminating the input. This is because the output-impedance formula (5) can be transformed into the form

$$(-Z_G) = Z_{11} - \frac{Z_{12}Z_{21}}{Z_{22} - Z_{\rm OUT}} \tag{15}$$

```
     ∇ RTN←UNTERMINATE A
[1]    N←(ρA)÷2
[2]    ZIN←N↑A
[3]    ZL←N↓A
[4]    AI←(+/ZIN)÷N
[5]    AL←(+/ZL)÷N
[6]    ALI←(+/ZL×ZIN)÷N
[7]    VI←(+/(|ZIN-AI)*2)÷N
[8]    VL←(+/(|ZL-AL)*2)÷N
[9]    VLI←(+/(ZL-AL)×CC(ZIN-AI))÷N
[10]   VLIL←(+/((ZL×ZIN)-ALI)×CC(ZL-AL))÷N
[11]   VLII←(+/((ZL×ZIN)-ALI)×CC(ZIN-AI))÷N
[12]   DENOM←(VL×VI)-(|VLI)*2
[13]   Z11←((VI×VLIL)-VLII×CC VLI)÷DENOM
[14]   Z22←((VLI×VLIL)-VL×VLII)÷DENOM
[15]   DELTAZ←ALI+(Z22×AI)-Z11×AL
[16]   RTN←Z11,Z22,DELTAZ
     ∇
```

```
     ∇ RTN←UNT A
[1]    N←(ρA)÷2
[2]    ZIN←N↑A
[3]    ZL←N↓A
[4]    ALPHA←ZL×ZIN
[5]    BETA←ZL,(-ZIN),[1,5] 1
[6]    RTN←ALPHA⌹BETA
     ∇
```

Fig. 6. Two algorithms to calculate Z_{11}, Z_{22}, and Δ_Z from $Z_{\rm IN}$ and Z_L values. The algorithms are intended for exposition, but can actually be executed if all Z_L and $Z_{\rm IN}$ are real. In this case the complex-conjugate indicated by CC is not necessary. The argument A is a vector containing the N values of $Z_{\rm IN}$ and the N values of Z_L, which are extracted in lines [1]–[3]. In APL the sum of all elements of a vector V is denoted by $+/V$; * denotes exponentiation; | denotes magnitude; and ← is used for specification. The function unterminate carries out in detail the calculations. The function UNT is a simplified version that does the same thing, making use of the APL matrix-inverse primitive function ⌹, which automatically finds a least square approximation solution to a set of overdetermined linear equations. Both functions produce the same result.

```
     ∇ RTN←FORS A
[1]    N←(ρA)÷2
[2]    MEAS←N↑A
[3]    LOADS←N↓A
[4]    RTN←MEAS,-1÷LOADS
     ∇
```

Fig. 7. A function to precondition reflection-coefficient data so that the functions UNT and UNTERMINATE can be used.

which has the same form as (1) provided $Z_{\rm IN}$ is replaced by $-Z_G$, and Z_L by $-Z_{\rm OUT}$. In fact, any combination of input and output measurements can be used.

Certain known facts about the embedding network can be incorporated in order to reduce the amount of measured data required. Two important practical cases are considered here, symmetry and losslessness.

For symmetric networks, $Z_{11} = Z_{22}$ and hence (7) becomes

$$Z_{11}(Z_{Li} - Z_{{\rm IN}i}) + \Delta_Z - Z_{Li}Z_{{\rm IN}i} = \epsilon_i. \tag{16}$$

At least two measurements are necessary, and if more than two exist, then the vector p'

$$p' = [Z_{11} \ \Delta_Z]$$

is found by solving (10), where now $\boldsymbol{\beta}^{*\prime}\boldsymbol{\beta}$ and $\boldsymbol{\beta}^{*\prime}\boldsymbol{\alpha}$ are smaller:

$$\boldsymbol{\beta}^{*\prime}\boldsymbol{\beta} = \begin{bmatrix} \sum_{i=1}^{N} |Z_{Li} - Z_{{\rm IN}i}|^2 & \sum_{i=1}^{N} (Z_{Li} - Z_{{\rm IN}i})^* \\ \sum_{i=1}^{N} (Z_{Li} - Z_{{\rm IN}i}) & N \end{bmatrix} \tag{17}$$

$$\beta^{*\prime}\alpha = \begin{bmatrix} \sum_{i=1}^{N} Z_{\mathrm{IN}i} Z_{Li} (Z_{Li} - Z_{\mathrm{IN}i})^* \\ \\ \sum_{i=1}^{N} Z_{Li} Z_{\mathrm{IN}i} \end{bmatrix}. \qquad (18)$$

For lossless networks, $Z_{11} = jX_{11}$ and $Z_{22} = jX_{22}$ and Δ_Z is real. Hence (7) can be split apart into a real and an imaginary part:

$$-X_{11}X_{Li} + X_{22}X_{\mathrm{IN}i} + \Delta_Z - \mathrm{Re}\, Z_{Li}Z_{\mathrm{IN}i} = \mathrm{Re}\, \epsilon_i$$
$$X_{11}R_{Li} - X_{22}R_{\mathrm{IN}i} - \mathrm{Im}\, Z_{Li}Z_{\mathrm{IN}i} = \mathrm{Im}\, \epsilon_i. \quad (19)$$

At least two general measurements are necessary (three if reactive loads are used), and if more exist, then the real vector p'

$$p' = [X_{11}\ X_{22}\ \Delta_Z]$$

is found by solving (10), where now $\beta^{*\prime}\beta$ and $\beta^{*\prime}\alpha$ are

$$\beta^{*\prime}\beta = \begin{bmatrix} \sum_{i=1}^{N} |Z_{Li}|^2 & -\sum_{i=1}^{N} \mathrm{Re}\, Z_{Li}^* Z_{\mathrm{IN}i} & -\sum_{i=1}^{N} X_{Li} \\ -\sum_{i=1}^{N} \mathrm{Re}\, Z_{Li} Z_{\mathrm{IN}i}^* & \sum_{i=1}^{N} |Z_{\mathrm{IN}i}|^2 & \sum_{i=1}^{N} X_{\mathrm{IN}i} \\ -\sum_{i=1}^{N} X_{Li} & \sum_{i=1}^{N} X_{\mathrm{IN}i} & N \end{bmatrix} \qquad (20)$$

$$\beta^{*\prime}\alpha = \begin{bmatrix} \sum_{i=1}^{N} \mathrm{Im}\, |Z_{Li}|^2 Z_{\mathrm{IN}i} \\ -\sum_{i=1}^{N} \mathrm{Im}\, |Z_{\mathrm{IN}i}|^2 Z_{Li} \\ \sum_{i=1}^{N} \mathrm{Re}\, Z_{Li} Z_{\mathrm{IN}i} \end{bmatrix}. \qquad (21)$$

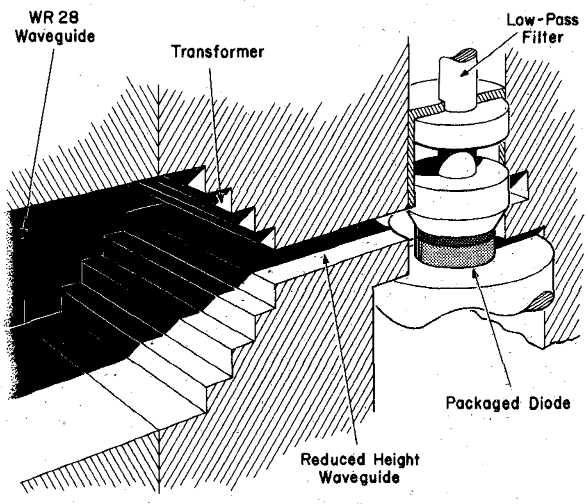

Fig. 8. Cut-away view of a 37-GHz IMPATT diode reflection amplifier circuit.

VIII. Example

In this section the unterminating procedure is illustrated by determining the impedance seen by the active region (the avalanche and drift regions) of an IMPATT diode. The diode is mounted as shown in Fig. 8 in a reflection amplifier circuit designed for operation at 37 GHz.

The reflection coefficient referred to the transformer–waveguide interface was taken as the input measurement. The junction capacitance of the diode for various bias voltages was used as the set of reference loads. Thus the embedding network includes the waveguide transformer, the reduced-height waveguide, the bias line, the backshort and mounting cavity, the diode package, and even a portion of the semiconductor.

As pointed out by Steinbrecher and Peterson [3], the depletion-layer capacitance should be independent of frequency well into the microwave region because of the small physical size of the junction and thus can be determined from measurements at much lower frequencies using a conventional capacitance bridge.

The microwave measurement of the input reflection coefficient was made with a slotted line. Eight measurements, corresponding to eight different bias voltages, were made. The data presented here are for measurements made at 37 GHz.

The estimated value of Z_{OUT} using all eight of the measurements to predict the network parameters was $24.3 + j31.8\ \Omega$. To show the possible error, the predicted values of Z_{OUT} using three measurements at a time are shown in Fig. 9. The mean and standard deviation of the estimated Z_{OUT} obtained by taking the measurement pairs 3–8 at a time are plotted in Fig. 10. This plot illustrates the decrease in the uncertainty associated with the estimated Z_{OUT} as the number of measurements is increased.

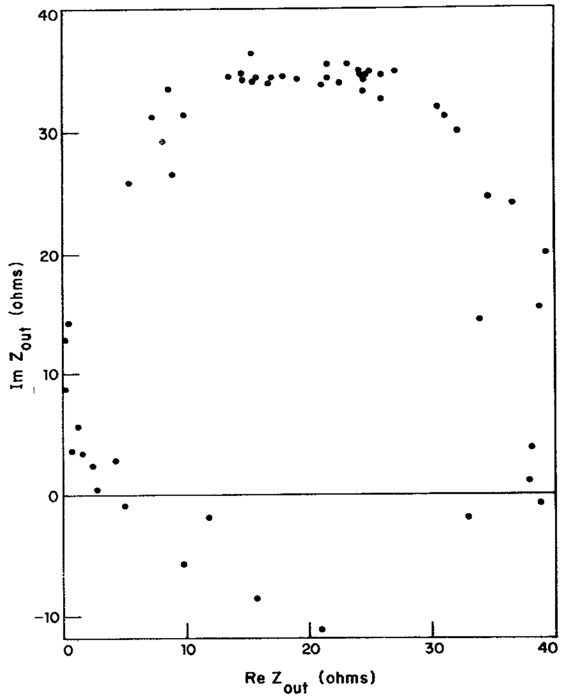

Fig. 9. Output impedances of the 56 different characterizations of the reflection amplifier obtained by using only 3 measurements at a time from the set of 8.

IX. Conclusions

A practical procedure has been shown for unterminating that makes effective use of more than the minimum number of measurements. The technique as presented applies to two-port embedding networks, with equal weightings on all measurements.

The extension to multiport embedding networks is probably straightforward. This would be required, for example, in coupling to a two-port device such as a transistor as described by Calahan [6].

Unequal weightings can easily be incorporated in the

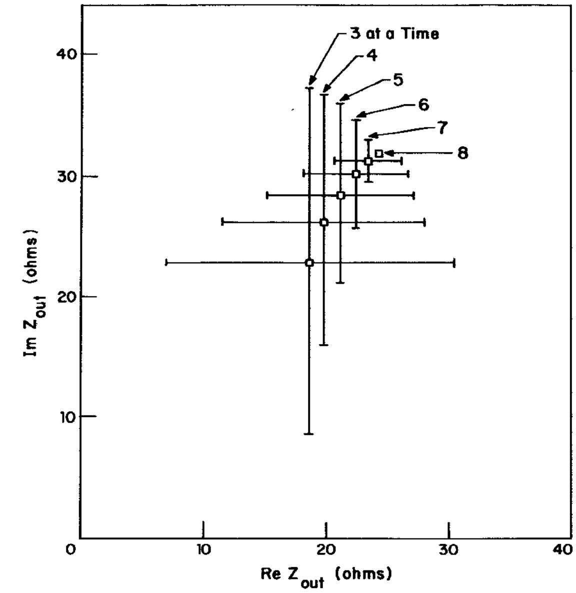

Fig. 10. Mean and standard deviation of the predicted output impedances obtained by taking 3–8 measurements at a time.

procedure, if desired. It is only necessary to multiply the appropriate elements of α and the appropriate rows of $\boldsymbol{\beta}$ by the desired weighting factors.

References

[1] P. Penfield, Jr., *MARTHA User's Manual.* Cambridge, Mass.: MIT Press, 1971.

[2] D. Kajfez, "Numerical data processing of reflection coefficient circles," *IEEE Trans. Microwave Theory Tech.*, vol. MTT-18, pp. 96–100, Feb. 1970.

[3] D. H. Steinbrecher and D. F. Peterson, "Small-signal model with frequency-independent elements for the avalanche region of a microwave negative-resistance diode," *IEEE Trans. Electron Devices*, vol. ED-17, pp. 883–891, Oct. 1970.

[4] C. N. Dunn and J. E. Dalley, "Computer-aided small-signal characterization of IMPATT diodes," *IEEE Trans. Microwave Theory Tech.*, vol. MTT-17, pp. 691–695, Sept. 1969.

[5] B. B. van Iperen and H. Tjassens, "Novel and accurate methods for measuring small-signal and large-signal impedances of IMPATT diodes," *Philips Res. Rep.*, vol. 27, pp. 38–75, 1972.

[6] D. A. Calahan, *Computer-Aided Network Design*, rev. ed. New York: McGraw-Hill, 1972, p. 43.